THE JOURNAL OF PHYSICAL CHEMISTRY B
A JOURNAL OF THE AMERICAN CHEMICAL SOCIETY

pubs.acs.org/JPCB

Article

Direct Measurement of the Selective Microwave-Induced Heating of Agglomerates of Dipolar Molecules: The Origin of and Parameters Controlling a Microwave Specific Superheating Effect

Published as part of The Journal of Physical Chemistry virtual special issue "Hellmut Eckert Festschrift".

Yuchuan Tao, Chong Teng, Terence D. Musho, Lambertus van de Burgt, Eric Lochner, William T. Heller, Geoffrey F. Strouse, Gregory B. Dudley,* and A. E. Stiegman*

Cite This: *J. Phys. Chem. B* 2021, 125, 2146–2156

Read Online

ACCESS | Metrics & More | Article Recommendations | Supporting Information

ABSTRACT: Agglomerates of polar molecules in nonpolar solvents are selectively heated by microwave radiation. The magnitude of the selective heating was directly measured by using the temperature dependence of the intensities of the Stokes and anti-Stokes bands in the Raman spectra of *p*-nitroanisole (pNA) and mesitylene. Under dynamic heating conditions, a large apparent temperature difference (ΔT) of over 100 °C was observed between the polar pNA solute and the nonpolar mesitylene solvent. This represents the first direct measurement of the selective microwave heating process. The magnitude of the selective microwave heating was affected by the properties of the agglomerated pNA. As the concentration of the pNA increases, the magnitude of the selective heating of the pNA was observed to decrease. This is explained by the tendency of the pNA dipoles to orient in an antiparallel fashion in the aggregates as measured by the Kirkwood *g* value, which decreased with increasing concentration. This effect reduces the net dipole moment of the agglomerates, which decreases the microwave absorption. After the radiation was terminated, the effective temperature of the dipolar molecules returned slowly to that of the medium. The slow heat transfer was modeled successfully by treating the solutions as a biphasic solvent/solute system. Based on modeling and the fact that the agglomerate can be heated above the boiling temperature of the solvent, an insulating layer of solvent vapor is suggested to form around the heated agglomerate, slowing convective heat transfer out of the agglomerate. This is an effect unique to microwave heating.

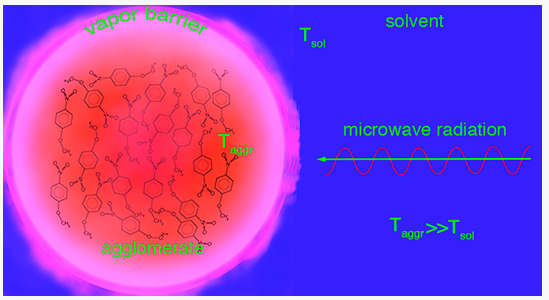

INTRODUCTION

There has been recent interest in the application of microwave radiation to drive chemical reactions, particularly in the area of synthetic organic chemistry.[1−5] This interest has been driven in large part because dramatic enhancements in reaction rates and product selectivity have been realized for certain chemical reactions.[2,6−8] In some cases, these enhancements are related simply to the rapid heating of a reactant/solvent system in a manner not possible with conventional thermal heating. In many other cases, claims of accelerated reaction rates, where the observed rates were much larger than what would be predicted from the Arrhenius equation for a particular temperature, were found to stem from improper temperature measurement inside the microwave cavity. The overidentification of microwave specific effects has been attributed to experimental difficulties in accurately measuring temperature within the reaction vessel. Subsequently, as the technology for accurately determining temperature in the microwave improved, studies of homogeneous reactions were reported that clearly showed microwave specific rate enhancement.[9−17]

As demonstrated by Stiegman and Dudley et al., a systematic analysis of microwave effects on a homogeneous chemical reaction was reported that allowed the magnitude of the microwave effect to be quantified under specific conditions of microwave heating. Specifically, the unimolecular first-order Claisen rearrangement of allyl *p*-nitrophenyl ether (ApNE) in a nonpolar solvent was examined under both microwave and conventional convective (thermal) heating. The rate constants as a function of temperature and the Arrhenius parameters were determined. By collection of kinetic data under microwave conditions and with accurate internal temperature measurements, the magnitude of the microwave enhancement could be quantified by comparing the rate constant observed

Received: November 15, 2020
Revised: February 5, 2021
Published: February 19, 2021

https://dx.doi.org/10.1021/acs.jpcb.0c10291
J. Phys. Chem. B 2021, 125, 2146–2156

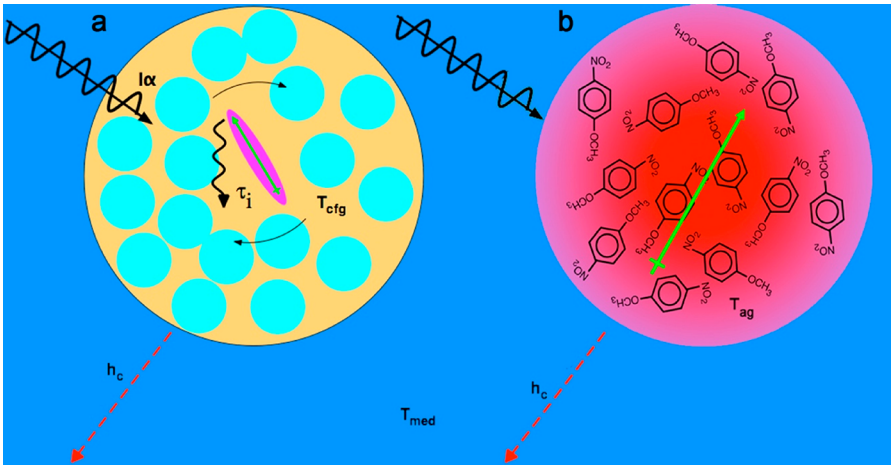

Figure 1. (a) Heat storage in domains surrounding a dipolar molecule, where T_{cfg} is the configurational temperate, T_{med} is the temperature of the medium, and τ_i is the relaxation time. (b) Selective heating of an agglomerate of dipolar molecules where T_{ag} is the apparent temperature of the agglomerate; the green arrow is the net dipole moment of the agglomerate. In both cases h_c is the convective heat transfer coefficient.

under microwave heating with the predicted value at the same temperature under thermal conditions. Under conditions of constant microwave power, reaching a temperature of 185 °C, a 4-fold rate enhancement was observed in the microwave over conventional heating; this means the microwave reaction was proceeding at an effective temperature of 202 °C. Under conditions of constant temperature, where the microwave adjusts the power to maintain a constant temperature, an ∼1.5-fold microwave-specific rate enhancement was observed at a set point temperature of 200 °C. The largest microwave-specific rate enhancement was observed by using a series of 300 W power cycles, programmed for 145−175 °C and 85−155 °C cycles, in which 2-fold and 9-fold rate enhancements were observed, respectively, compared to conventional thermal heating. The power cycle−heating method thus resulted in a large microwave enhancement effect. This is important from the standpoint of potentially providing a general approach to microwave heating that can achieve results in solution-phase organic reactions that cannot be obtained by using conventional heating.

The hypothesized origin of the microwave-specific enhancement is purely thermal and arises from selective heating of ApNE, a microwave-absorbing solute in a nonabsorbing solvent. Under these conditions, excess heat is accumulated in the domains of the ApNE solute so that it experiences a higher effective temperature than the measured temperature of the bulk medium, resulting in an accelerated unimolecular rearrangement. More generally, if a highly absorbing molecule is present as a solute in a nonabsorbing solvent, the heat gained by the entire solution must arise from selective absorption of microwave energy leading to latent heating of the solute. The solute heats the surrounding solvent through a combination of convective and radiative heat flow into the solvent and out of the system at the boundaries. As will be discussed, a thermal contact layer is critical to maintaining the finite and persistent thermal gradient between the solute and the solvent. Under these conditions, the absorbing molecule will act as a "thermophore" or, as it has also been termed, a "molecular radiator", converting electromagnetic energy to heat through dipole relaxation.[18−20] If the thermophore is a reactant in a chemical transformation, based on the temperature dependence of the Arrhenius activation energy and pre-exponential term, it is reasonable to assume faster reaction rates will be realized.[21]

The model for the storage of heat around an absorbing dipole comes from the elegant dielectric relaxation work of Richert.[22,23] In the model, domains are well-defined chemically by the dipolar molecule and the solvation sphere around it, as illustrated schematically in Figure 1a.[24] Such discrete domain formation is similar to heterogeneous domains formed in pure liquids because a small subset of the sample will absorb a majority of the power in a spatially heterogeneous fashion. As illustrated in Figure 1a, the microwave radiation couples with the permanent dipole moment, which experiences a rotational torque due to the oscillating incident field. The amount of energy absorbed by a domain will depend on the microwave flux and the absorption cross section of the domain, Iα, at a given frequency (2.45 GHz).

Within the domain depicted in Figure 1a, dielectric loss occurs through the configurational relaxation that accompanies the reorientation of the dipole within the solvent shell. These configurational relaxation processes occur with time constants τ, which, for this type of configuration relaxation, is inherently slow. The fact that the frequencies of microwave radiation excite configurational modes that relax slowly distinguishes it from conventional heating in that the direct transfer of heat to the rapid (predominantly vibrational) phonon modes of the medium is inherently inefficient (i.e., small convective heat transfer coefficient, h_c). As such, heat will accumulate within the configurational domain, giving the molecules contained within it a temperature (T_{cfg}) that can be larger than that of the surrounding medium (T_{med}).

For a collection of dipolar molecules in a nonpolar solvent, the idealized model of an isolated molecule oscillating in a solvent shell as depicted in Figure 1a is unrealistic. Under these conditions, the dipoles interact and the molecules form agglomerates with each other via dipolar (polarizability), molecular (van der Waals, H-bonding, π-stacking, and electrostatic), and interfacial effects (Figure 1b). These agglomerates, surrounded by the nonpolar solvent, define the domain of the system that is heated by incident microwave radiation. Microwave heating of the agglomerate is governed by the loss tangent of the agglomerate domain, which is related to the net dipole moment of the total agglomerate.[25] As such,

https://dx.doi.org/10.1021/acs.jpcb.0c10291
J. Phys. Chem. B 2021, 125, 2146−2156

heat will accumulate within the configurational domain, giving the molecules contained within it a temperature (T_{cfg}) that can be larger than that of the surrounding medium (T_{med}). The higher the configurational temperature relative to the measured temperature of the bulk medium, the more pronounced the specific microwave acceleration effect should be providing one or all of the absorbing species is a reactant. The transfer of heat out of the domain (h_c in Figure 1b) will depend on a number of parameters, including the nature of the interface between the agglomerate and the solvent. This of particular interest as the temperature of the polar solute agglomerate quickly reaches the vaporization temperature of the nonpolar (and typically lower boiling) solvent.

In this study we will analyze the origin of the microwave enhancement under pulse heating conditions. Unlike the conditions of constant power and temperature, where the temperature is at steady state or held constant by the instrument, pulse heating is a dynamic process where heat is rapidly being absorbed by the dipolar molecule. In this study we measure, for the first time, the effective temperature of the dipolar molecules during the dynamic heating using Stokes/anti-Stokes Raman spectroscopy.

METHODS

The reagents *p*-nitroanisole (pNA), mesitylene (MES), and mesitylene-d_{13} (98 atom %) were obtained from Aldrich and used as received. Solutions of pNA in MES at mole ratios of 1:20, 1:10, and 1:5 were prepared for the experiments. Microwave heating of 2 mL aliquots of the series of solutions was performed in CEM SP microwave in quartz reaction tubes.

Raman spectra of the solutions during dynamic heating in the microwave cavity were performed by directing a 488 nm line at a power of 1 W from an argon ion laser through the CEM SP's available port. The Stokes and anti-Stokes Raman scatterings were collected through a notch filter to reject the laser line. The effective temperature was determined from the intensities of the Stokes and anti-Stokes Raman bands (see the Supporting Information).

Temperatures during power cycling of the microwave were collected on the series of pNA/MES samples, 2 mL in quartz tubes, in a CEM SP microwave with the temperature monitored internally by a fiber-optic integral to the CEM. In these experiments, the solution is heated from room temperature at a fixed power of 300 W. Once the high-temperature limit is attained, the microwave power ceases, and the solution cools to the lower temperature limit. This process is repeated for the duration of the experiment.

Static dielectric measurements were performed in a solution cell fabricated from a published schematic.[26] The static dielectric constant was measured on an HP 4284A LCR meter. The instrument measures LCR (inductance, capacitance, and resistance) in serial and parallel configurations from 20 Hz up to 1 MHz. A signal of specified frequency, amplitude, and DC offset is applied to the sample, and the corresponding complex impedance is used to measure the effect LCR values. The dielectric constant at an infinite frequency (ε_∞) was obtained from the refractive index collected at 546 nm with an Abbe refractometer (NAR-4T) at 20 °C.

RESULTS AND DISCUSSION

To investigate the selective heating of dipolar molecules in solution, we use highly absorbing dipolar nitroaromatic probe molecules dissolved into dilute solutions with nonpolar aromatic solvents, specifically, *p*-nitroanisole (pNA) in mesitylene (MES). This system replicates the physical characteristics and the microwave heating properties of the ApNE (allyl *p*-nitrophenyl ether) reaction system studied previously, but it maintains a constant composition since no reaction is taking place.[27] A series of solutions investigated having pNA:MES mole ratios of 1:20, 1:10, and 1:5 were investigated for their heating properties under conditions of dynamic microwave heating.

Nature of the *p*-Nitroanisole:Mesitylene Solutions. As discussed, the dipolar molecules are not individually solvated by the nonpolar solvent but are associated through dipole−dipole interactions to form agglomerates of the absorbing species, in this case pNA. The surface tension of these agglomerates presumably results in predominantly spherical domains of dipole molecules. The effects of the agglomeration of dipolar molecules on microwave heating and dielectric properties were discussed in a detailed in a study by Horikoshi et al. of ethanol molecules dispersed in the nonpolar solvents, specifically benzene or *n*-dodecane.[28] In that study, it was demonstrated that the dipole−solvent combination affects the heating rate in the microwave. As expected, the heating rate increased with increasing ethanol concentration; however, distinct differences were observed between ethanol−benzene and ethanol−*n*-dodecane solutions. In particular, the heating rate of the ethanol−benzene solution is more rapid at lower ethanol concentrations than the ethanol−*n*-dodecane mixtures. This is attributed to differences in the degree of association of the ethanol in the two different solvents. The hypothesis was supported by measurement of the real and imaginary dielectric constants of the two solutions as a function of concentrations and by the measurement of the interaction of the dipoles with each other in the solution using the Fröhlich equation.

The association of dipolar molecules in a nonpolar solvent was exploited to heat molecules that heat only modestly in the microwave through association with molecules with higher dipole moments—an effect termed the chaperone effect.[29] In that study, Claisen rearrangements of allyl phenyl ether in tridecane solvent were examined with and without 1-nitronaphthalene as a polar additive. Without added 1-nitronaphthalene, allyl phenyl ether in tridecane did not undergo Claisen rearrangement under microwave heating at any appreciable rate because appropriate solution temperatures could not be achieved. With added 1-nitronaphthalene, the Claisen reaction was found to proceed in part because temperatures commensurate with this reaction were obtained, but it was determined that the reaction rate was significantly higher than what would be predicted from the measured temperature of the solution. This is an important finding as it indicates that an agglomerate comprising both allyl phenyl ether and 1-nitronaphthalene can function as a domain that can store heat that is greater than the bulk temperature.

These aforementioned studies provide evidence of microwave effects in solutions of dipolar molecules in nonpolar solvents. Leading contributors to these enhancements are the dipole−dipole interactions with the agglomerates. To quantify the heat storage properties of the pNA:MES compositions, it necessary to confirm the presence of an agglomerate phase and to estimate the size of the agglomerates in at various pNA concentrations in solution.

Small-Angle Neutron Scattering (SANS). The presence of the pNA agglomerates was detectable by SANS. Solutions of

https://dx.doi.org/10.1021/acs.jpcb.0c10291
J. Phys. Chem. B 2021, 125, 2146−2156

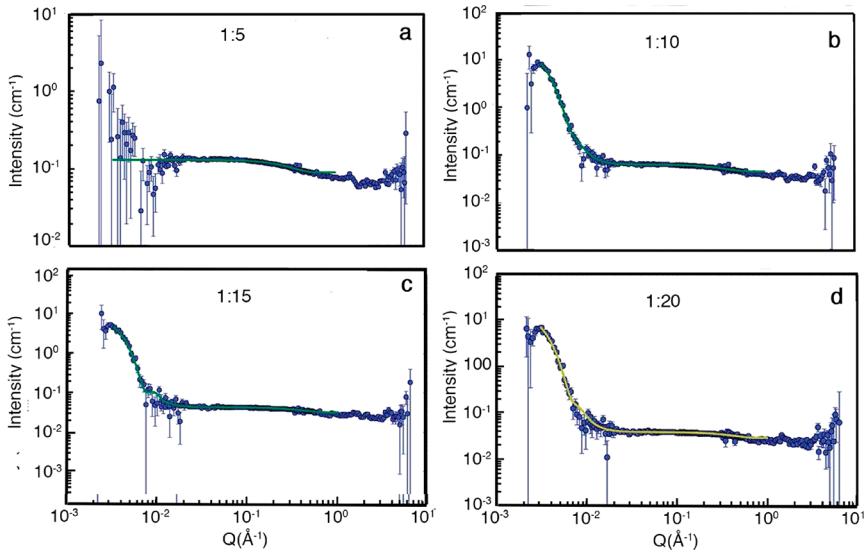

Figure 2. Small-angle neutron scattering data for a series of pNA:mesitylene concentrations. The solid lines are fits to the data using a model having two different sizes of spheres (1:10, 1:15, and 1:20) or a single size of sphere with a structure factor to account for interparticle interference effects (see the Supporting Information).

pNA were dissolved in deuterated mesitylene (*d*-mesitylene) at PNA:MES ratios of 1:5, 1:10, 1:15, and 1:20. The use of *d*-mesitylene in the measurements provided scattering length density contrast to make it possible to observe any pNA structures. The SANS data collected for the series are shown in Figure 2 with experimental details given in the Supporting Information.

For the 1:10, 1:15, and 1:20 samples, the SANS (Figure 2b–d) data show clear indication of large structures, while the 1:5 sample (Figure 2a) lacks this feature. The signal quality in the low-Q region of the SANS data of the 1:5 sample is the result of the lack of the large structures present in the other samples that scatter sufficiently strongly to make up for the lower neutron flux of the instrument configurations that provide this portion of the data (see the Supporting Information). Guinier plots of the scattering data in the $QR_g < 1.0$ region (Figure 3)

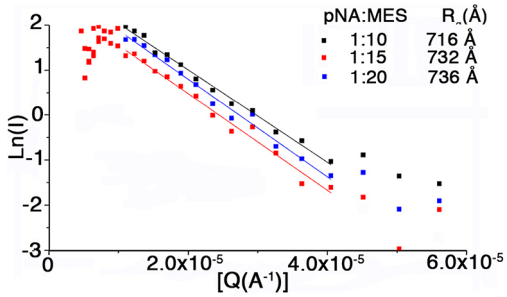

Figure 3. Guinier plots of the SANS data for the series of pNA:MES concentrations.

show good linearity for the three lowest pNA concentrations. Least-squares fits yield radii of gyration of 716, 732, and 736 Å for 1:10, 1:15, and 1:20, respectively. The SANS data of the 1:5 sample cannot be fit in this manner in this Q-range. The results indicate that the structures adopted by pNA change as the system approaches an equimolar mixture. It is interesting to note that all samples show evidence of small structures because the data are not flat in the high-Q regime. This feature is most prominent in the 1:5 sample.

The SANS data were fit by using a hard-sphere model either with two different size spheres or with a single sphere size. The resulting model curves are shown in Figure 2. The two-sphere model fits the three lowest concentration SANS data sets well (Figure 2a–c). Consistent with the Guinier analysis, the largest particles are around 600 Å (Table 1). The smaller sphere has

Table 1

pNA:MES	sphere 1 radius (Å)	sphere 2 radius (Å)
1:20	587.00 (±59.82)	3.19 (±0.05)
1:15	618.47 (±22.35)	3.07 (±0.06)
1:10	581.32 (±30.54)	3.22 (±0.02)
1:5	6.50 (0.07)	

an unphysical size, and the feature may be due to artifacts arising from inelastic scattering.[30] The fit of the data set collected at the highest concentration (1:5) by using a model with a single size of sphere and an applied a structure factor to account for the likely interparticle interactions in such a concentrated system revealed no large structures as are observed for the lower concentrations of pNA but instead smaller structures suggestive of clusters. The volume of the sphere (1150 Å^3) is large enough for 5–6 pNA molecules ($V_{pNA} \sim 203$ Å^3).

Determination of Dipole–Dipole Interactions in the Agglomerates. The dipole moment of pNA is 4.78 D computed by using the Guggenheim method from the measured static dielectric constants and refractive indices of dilute solution of pNA in MES (see the Supporting Information).[31,32] We note that the value of dipole moment determined from a dilute solution where the dipolar molecule is solvated by the nonpolar solvent will depend on specific interactions with the nonpolar solvent and therefore be different from the value in other solvents or in the gas phase.[26,33]

Measurement of dipole–dipole interactions of the dipolar molecules in nonpolar solvents is determined from calculation of the effective dipole moment, $g\mu^2$, using the Onsager–Kirkwood–Fröhlich equation:

https://dx.doi.org/10.1021/acs.jpcb.0c10291
J. Phys. Chem. B 2021, 125, 2146–2156

$$g\mu^2 = \frac{9kT\varepsilon_0(2\varepsilon + n^2)^2}{N_A X_2(n^2 + 2)^2(2\varepsilon + 1)}\left\{\frac{\varepsilon + 1}{\varepsilon}\left[\frac{X_1M_1 + X_2M_2}{d}\right] - \frac{3X_1M_1(\varepsilon_1 - 1)}{d_1(2\varepsilon + \varepsilon_1)} - \frac{3X_2M_2(n^2 - 1)}{d_2(2\varepsilon + n^2)}\right\} \quad (1)$$

where ε, d, and n are the permittivity, density, and refractive index of the solution, respectively, while ε_1, ε_1, M_1 and ε_2, ε_2, M_2 are the mole fraction, permittivity, and molecular weight for the solute and solvent, respectively. The Kirkwood factor, g, which is obtained by dividing $g\mu^2$ by the dipole moment of the polar molecule, can be obtained at low concentration. The value of g indicates dipole−dipole interactions between the polar molecules.

If $g > 1$, the dipole moments of the molecules are aligned in a parallel fashion, while for $g < 1$ the molecules are aligned antiparallel (Figure 4). Dielectric constants and the refractive

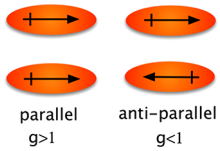

Figure 4. Parallel and antiparallel intermolecular dipole−dipole interactions leading to values of the Kirkwood factor, g, greater and less than one, respectively.

indices were measured for pNA/mesitylene solutions over the range of concentrations investigated in the study. The Kirkwood g factor was calculated and plotted in Figure 5.

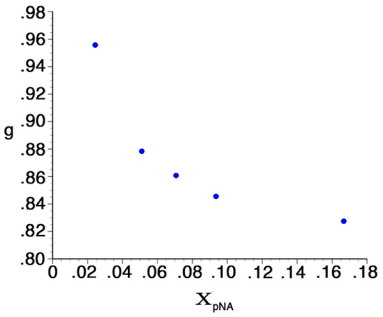

Figure 5. Values of the Kirkwood factor, g, as a function of the mole fraction of pNA in MES.

As is apparent in Figure 5, the g value decreases rapidly as a function of the mole fraction of pNA. This suggests that as the pNA concentration increases, agglomeration results in significant amount intermolecular dipole−dipole interactions in an antiparallel orientation. This will affect the heating properties of the solution since the coupling of the radiation with the agglomerate will be through the net dipole moment of the agglomerates, not the individual molecules in the agglomerates (Figure 1b). Furthermore, as seen in Figure 5, as the pNA concentration increases, there is a leveling off of the g value. This indicates either that larger agglomerates lose their shape at high concentration, as was the case for 1:5, or that there is an equilibrium antiparallel concentration.

Modeling of the Agglomerates. The agglomerates were modeled in COMSOL Multiphysics simulation software in a multiscale modeling approach. In the study, two length scales of models were defined. The first model is a macroscale model that captures length scales at $0.1-1\lambda_{2.45GHz}$. More specifically, the macroscopic models explicitly modeled the CEM microwave system, which includes the waveguide geometry, location of the magneton source, and a quartz tube with effective specimen properties. The second model is a microscale that models a single agglomerate in a periodic box. The microscale model is aimed at capturing subwavelength physics in a full wave treatment of the electromagnetic interactions. A detailed model setup and description can be found in the Supporting Information.

The macroscopic model involved a coupled multiphysics simulation that solved the electromagnetic, heat transfer, and laminar fluid flow. The microscopic model involved solving the electromagnetic and heat transfer coupled solution similar to previous studies.[34] The microscale model assumed that the bulk motion was negligible. In modeling both scales it was found critical to consider several heat transfer aspects to get the correct time history temperature response when comparing to the experiment. Those aspects included (1) temperature-dependent dielectric and thermal diffusivities, (2) radiation heat transfer with correct view factors, and (3) convective driven flow.

Direct Measurement of Temperature in Microwave-Heated Agglomerates. The origin of microwave-specific rate enhancement is hypothesized to be a result of selective absorption of MW energy by agglomerates of polar modules in nonpolar solutions leading to increased latent heating. The hypothesis is well supported by kinetic studies of solution reactions. What has been lacking is a direct measure of the temperature of the absorbing species and how that energy is dispersed into the medium.[9−11,27,29] The temperature inside the agglomerates can be analyzed via Raman spectroscopy methods through the ratio of the Stokes and anti-Stokes Raman scattering.[35,36] Spectra collected for a 1:10 pNA:MES solution are shown in Figure 6.

The temperature is determined for the molecular species from the relative intensity of the Stokes/anti-Stokes bands (I_s/I_{as}) by using eq 2[37]

$$\frac{I_s}{I_{as}} = \frac{(\nu_0 - \nu_k)^4}{(\nu_0 + \nu_k)^4} e^{hc\nu_k/kT} \quad (2)$$

where ν_0 and ν_k are the frequencies of the incident radiation and the vibrational modes being observed, and h, c, and k have their usual definitions. For accurate temperature determination, the choice of vibrational modes to monitor is important. Moreover, to observe a transition in both the Stokes and anti-Stokes regime, the transition must be discernible, which due to the nature of the Boltzmann distribution will require a low vibrational frequency. For the accurate use of eq 2, the vibrational mode must also be nondegenerate. In practice, symmetric fundamental stretching modes are the most reproducible. For pNA the symmetric NO_2 stretching mode is at 1332 cm^{-1} while for the mesitylene solvent a C−C stretch is at 579 cm^{-1}. Full details on the experimental setup, data collection, and analysis are provided in the Supporting Information.

Agglomerate Temperature as a Function of Concentration. The temperatures of the pNA absorber and the nonabsorbing MES solvent were determined from the Raman spectra at three different concentrations. The effective temperatures calculated from the spectra over the course of active heating in the applied microwave field and subsequent

https://dx.doi.org/10.1021/acs.jpcb.0c10291
J. Phys. Chem. B 2021, 125, 2146−2156

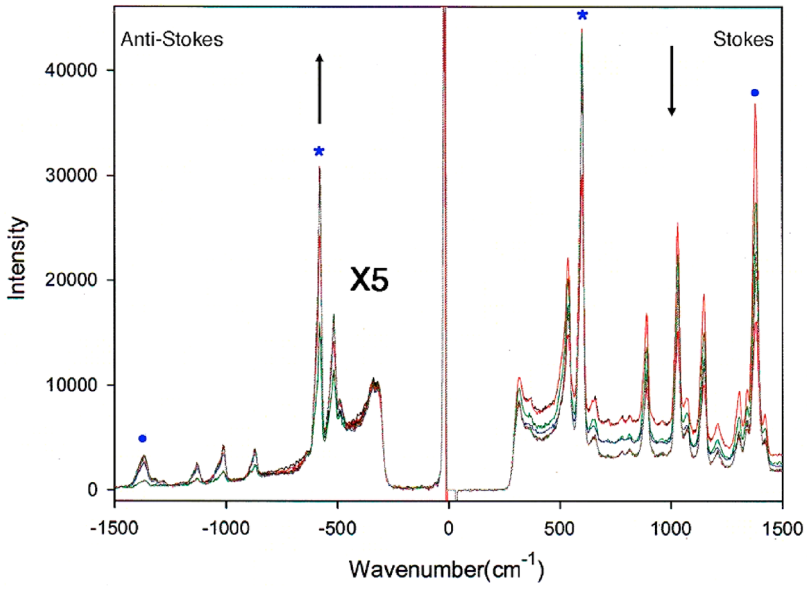

Figure 6. Raman spectra of a 1:10 mole ratio solution of *p*-nitroanisole:mesitylene collected as a function of temperature under microwave irradiation at 300 W. Bands monitored for temperature calculation for the *p*-nitroanisole (●) and mesitylene (∗) are indicated in the spectra. The arrows indicate the intensity change in the spectra as the temperature increases.

cooldown in the absence of the microwave field at three different mole fractions of *p*-nitroanisole are shown in Figure 7a–c. As is apparent from the data, the measured temperature difference between the pNA and the MES solvent is significant,

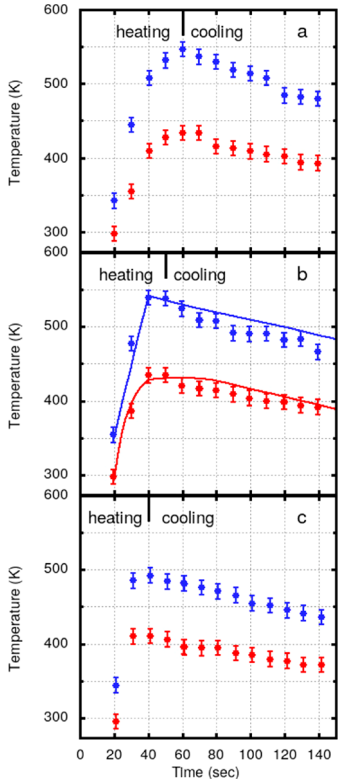

Figure 7. Measured temperature of (blue ●) *p*-nitroanisole and (red ●) mesitylene of (a) 1:20, (b) 1:10, and (c) 1:5 mole ratio of *p*-nitroanisole:mesitylene as a function of 300 W microwave radiation time. Microwave radiation was applied until the boiling point of the solution was reached (ca. 165 °C or 438 K). Solid lines are temperatures calculated from the COMSOL FEA model.

suggesting a pronounced selective microwave heating effect. Moreover, the maximum temperature attained by the pNA and the temperature difference between it and the MES change as a function of concentrations. The largest value for the temperature difference was observed for the most dilute solution (Figure 7a), where at the end of the heating cycle the pNA has an effective temperature of 272 °C, with a temperature difference (ΔT) between it and the MES solvent of 114 °C.

Figure 8 shows the maximum values attained by each component at the end of the heating cycle. There is a general

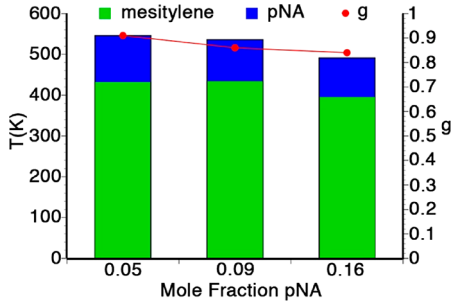

Figure 8. Apparent temperature of the mesitylene solvent (green) and the *p*-nitroanisole dipolar aggregates (blue) as a function of the mole fraction of *p*-nitroanisole. The Kirkwood *g* values for each composition are shown in red.

decrease in the temperature reached by the pNA agglomerates as a function of concentration. This trend correlates with the decrease in the Kirkwood factor with increasing concentration, which reduces the dipole moment of the agglomerate and, hence, the imaginary part of the dielectric constants, ε'', so that less radiation is absorbed into the individual agglomerates.

What is also observed is as the concentration of pNA increases, the rate of heating of the solution also increases. In particular, the heating rate estimated from the first few points of the heating curve are 0.08, 0.10, and 0.12 deg/s for 1:20, 1:10, and 1:5 pNA:mesitylene compositions, respectively. Because the size of the agglomerates for 1:20 and 1:10 are

https://dx.doi.org/10.1021/acs.jpcb.0c10291
J. Phys. Chem. B 2021, 125, 2146–2156

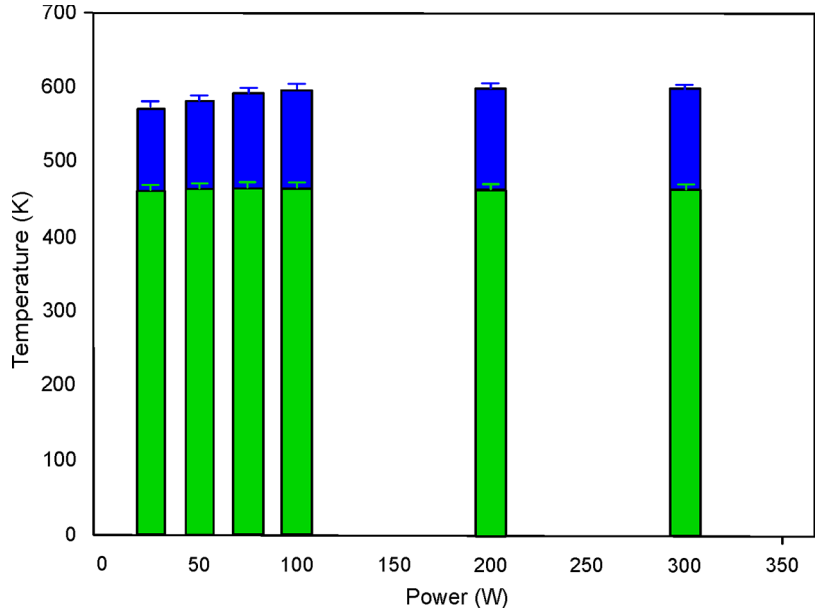

Figure 9. Measured temperature of the 1:10 mole ratio of (blue) *p*-nitroanisole to (red) mesitylene as a function of microwave applied power.

similar (Table 1), the enhanced heating rate can be ascribed to a larger quantity of agglomerates in the solution. For the 1:5 pNA:mesitylene large structures are not observed or are outside the detection limit which has taken its scattering signal outside the *Q*-range measured (on the low-*Q* side). Because the solution is transparent, this is unlikely; the data indicate that small structures are present, as evidenced by the very noisy data in that *Q*-range for that sample, which is consistent with the low scattering power that results from small structures. The pNA is still surrounded by mesitylene, meaning that there are a lot of interfaces where vapor can form (Figure 10), but they are smaller and constrained due to the relative volume fractions. This is consistent with the smaller heating difference between the pNA and the mesitylene observed for this system.

Agglomerate Temperature as a Function of Applied Power. The effect of the incident microwave power on the configurational temperature of the *p*-nitroanisole absorber in the mesitylene medium is shown in Figure 9. As can be seen, as the power increases, there is an increase in ΔT that is brought about almost exclusively by an increase in the temperature of *p*-nitroanisole. The increase in temperature is linear with applied power until a power of ∼100 W is reached, at which point the system reaches thermal saturation and there is no further increase in ΔT. The power dependence arises from the progressively more rapid absorption of energy by the agglomerates with increasing power. The heat stored in the agglomerate will be determined by the balance of the rate of radiation absorption with the heat loss out of the agglomerate. A detailed analysis of the heat flow in the system is provided in the next section. The observed saturation likely occurs when the incident radiation flux exceeds the ability of the aggregates to absorb more energy.

Modeling of the Heat Transfer Process. An important observation from the temperature data provided in Figure 7 is that once the microwave is cut off, and the solution begins to cool, the time it takes for the pNA return to converge on the temperature of the mesitylene is quite long. In fact, for all of the solutions the effective temperature of the pNA and the mesitylene have not converged at 100 s after radiation cutoff. The relatively slow decrease in temperature of the pNA arises from slow heat transfer from the aggregates to the solvent. Notably, the temperature difference (ΔT) between the pNA and the mesitylene at the end of the measurement (140 s) decreases as a function of PNA concentration showing a ΔT of 88, 73, and 64 K at 1:20 for 1:20, 1:10, and 1:5 pNA:mesitylene compositions, respectively. This may occur because a larger number of pNA agglomerate will more rapidly transfer heat to the solvent due to the increase in surface area.

To confirm the influence of the increased temperature of the agglomerates, a series of finite element simulations were conducted that couple the electromagnetic results to heat transfer. The solid line in Figure 7b is a result of the simulation. To match the experimental data, there were two aspects that needed to be considered. The first aspect requires radiative heat transfer to be considered with the correct view factor. The second aspect is to explain the slow thermal relaxation time (>100 s). In order for the simulations to reproduce this slow thermal relaxation time, there needs to be a thermal conductance insulation layer around the agglomerates: i.e., a solvent vapor barrier surrounding the agglomerates as a result of partial vaporization of the solute from the agglomerate being at temperature above the boiling point of the solvent (mesitylene bp = 165 °C). As is evident in Figure 7, while the temperature of the solvent remains below the boiling point, the temperature of the agglomerate can attain much higher temperatures. It is reasoned, therefore, that there is vaporization at the interface that can be seen by the nonlinear response of the experimental temperature. During partial vaporization, energy is lost to latent heat of vaporization of the fluids. There are also additional heat-transfer physics happening that can lead to nonlinear temperature response. A schematic representation of this process is given in Figure 10.

Two other aspects considered in the simulation were the temperature-dependent dielectric properties and radiative heat transfer to the surroundings, both nonlinear effects to the temperature. However, the temperature response of the simulation during heating was close to linear, indicating that vaporization was taking place, which was not considered in the

https://dx.doi.org/10.1021/acs.jpcb.0c10291
J. Phys. Chem. B 2021, 125, 2146−2156

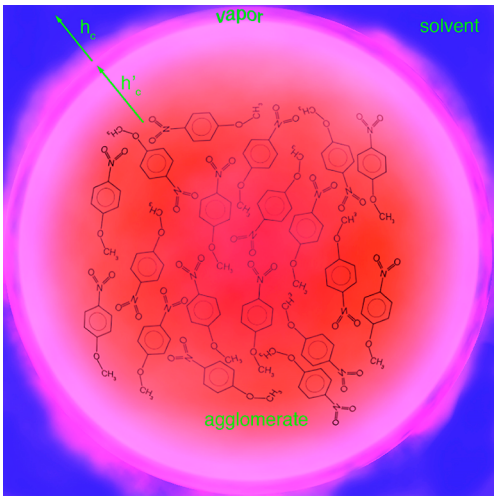

Figure 10. Schematic illustration of microwave-heated agglomerate showing the vapor barrier that forms and heat transfer from the agglomerate to the vapor barrier and then to the solvent.

simulation explicitly but rather considered implicitly by applying a thermal conductance insulation layer. The thermal contact resistance was necessary to account for the thermal impedance that arrives from the presents of the vapor layer. While this vapor layer is assumed to be thin, it was not explicitly modeled but accounted for at the boundary of the particle through a contact resistance. This contact resistance was necessary to maintain the thermal gradient between the *p*-nitro and mesitylene and in the absence of this layer the heat quickly dissipated from the *p*-nitro particle.

One aspect not considered in the microwave scale model is any nonlinear heat transfer associated with bulk motion (convection) in the solvent or solute. In the microscale model, the solvent and solute are treated as solids in the absence of advection. An additional consideration that should be addressed is the length scale. At length scales approaching nanoscale dimensions, quantum mechanical considerations of heat transfer must be applied. These considerations are not captured in the continuum heat transfer model. Typically, these quantum mechanical considerations are relevant when the mean free path of the phonons is on the length scale of the material features. A figure illustrating the microscale COMSOL model can be found in the Supporting Information.

The heat transfer physics at the scale of interest parallels many studies dealing with nanofluids or fluids with nanoparticles. A common claim in these nanofluid studies is that both metallic and nonmetallic nanoparticles enhance heat transfer in a convective fluid.[38] One study investigated gold and silver nanoparticles coated with thiolate and citrate in a toluene-based fluid;[39] it was found that the thiolate-coated particles had lower thermal conductivity enhancement. In drawing a comparison to this study, the nanoparticles are analogous to the agglomerates, which are the heat generation centers. The "coating" on the agglomerates is vaporized solvent species, which decrease the thermal conductance from the agglomerates to the bulk solvent. The retention of heat in the agglomerate domain here due to formation of a vapor layer is specific to the physics of selective microwave heating. This observation highlights a phenomenon not previously recognized but with great potential for strategic application in microwave chemistry.

Based on these aforementioned observations, conclusions, and discussion, it is reasonable to hypothesize that there would not be (could not be) any significant heat storage in a pure polar solvent, beyond the solvent heat capacity, which is consistent with the results of a recent study that found no selective heating effects in neat dimethyl sulfoxide solvent by using an experimental protocol similar to ours.[15] As such, the heating enhancements and response of the agglomerates will be strongly dependent on the concentrations of the absorbing and nonabsorbing components and will diminish as the concentration of the absorbing species increases in response to the increased size of the agglomerates and subsequent decreases in surface area.

Power Cycle Heating and Heat Dissipation in Polar/Nonpolar Solutions. The slow release of heat from the agglomerates can be observed in the temperature profile of the agglomerate solution during pulsed heating. In this pulsed experiment the solution is heated from room temperature at a fixed power. Once the set point temperature is attained, the microwave power is cut off and the solution cools convectively back down to a lower set point temperature. Once the lower temperature is attained, the microwave power is reapplied, and the solution is heated rapidly to the higher set point temperature.

This process is performed automatically by the CEM microwave with thorough stirring and measurement of the temperature internally by a calibrated fiber-optic thermometer. A pulse sequence performed between 80 and 120 °C at 300 W applied power was carried out on a 1:20 pNA:MES solution shown in Figure 11. There are several important aspects of the

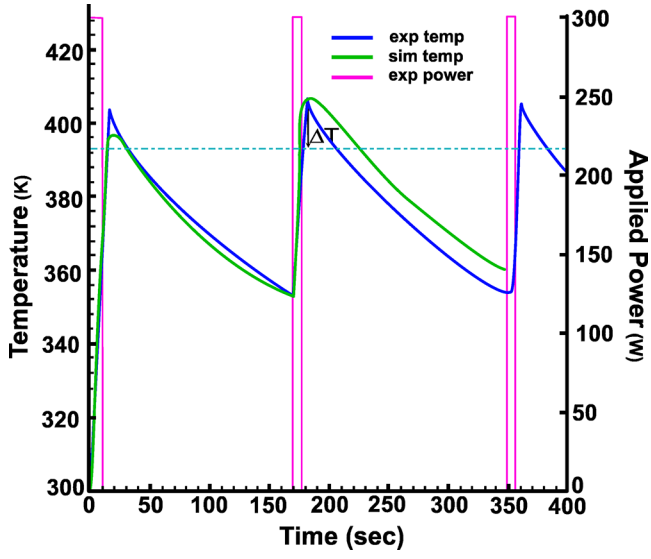

Figure 11. Experimental (blue line) and simulated (green line) temperature within specimen at upper and lower set point temperatures of 80 and 120 °C. The microwave was pulsed with power (magenta line) of 300 W, and the specimen was a 1:20 pNA:mesitylene solution.

plot. The period of the pulses is very reproducible, particularly in the early stages of the heating process. What is notable about the data is that when the upper limit of temperature is reached and power ceases, which occurs on the millisecond time scale, the bulk temperature continues to rise. Our hypothesis is that the observed temperature overrun is due to the storage and slow release of heat from the agglomerate.

https://dx.doi.org/10.1021/acs.jpcb.0c10291
J. Phys. Chem. B 2021, 125, 2146−2156

The blue line in Figure 11 is associated with the experimental fiber-optic temperature measurement, and the red line shows the duration that the power is applied during the pulse. The green line is associated with the macroscopic COMSOL model. Details on the simulation setup can be found in the Supporting Information. As can be seen in Figure 11, the primary features and, in particular, the temperature overrun are seen in the simulation data and are reasoned to be due to the nonequilibrium heating of the sample and the thermal capacitance of the sample. As can be seen in Figure S2, the peak temperature is not at the centroid of the sample but is offset. This is a result of the nonsymmetric radial waveguide of the CEM system.

Experimentally, temperature measurement was done by using a calibrated fiber-optic probe which is centered in the sample, though no effort was made to optimize the position at the highest temperature. To match the simulation time history with the experiment, it was necessary to sample an array of points within the specimen that represent possible points that the optical thermometer is situated within the solution. The simulation curve in Figure 11 is at a location of 4.5 mm from the bottom of the test tube. The simulated temperature at 20 locations can be found in the Supporting Information.

Detailed analysis of the simulation results determined that the temperature time history is very sensitive to the location that the temperature measurement was taken. This can be seen in Figures S4−S6 where, depending on the location, the cooling rate and response change. However, it was noted from the experimental curve in Figure 10 that the peak temperature point after the pulse has a high curvature (sharp point). However, the simulated point has a much lower curvature. It is possible some of this deviation may be due to the location of the thermometer or movement of the thermometer. It is hypothesized to be due either to the sample being stirred, which is not captured in the simulation, or to the surface tension and gathering of the pNA agglomerates on the tip of the optical thermometer.

CONCLUSIONS

Agglomerated polar solutes can be heated selectively in nonpolar solvents by using microwave heating, and the temperature differences between the polar agglomerates and the nonpolar bulk solvent can be large. Previous work has shown that reaction kinetics of solutes in the heated agglomerates can be accelerated relative to the measured bulk solution temperature and that these specific microwave effects can be most pronounced under dynamic heating conditions with on/off cycles of applied microwave power. Here we characterized agglomerates of pNA in mesitylene at different concentrations, and we determined the magnitude of selective heating spectroscopically using the temperature dependence of the intensities of the Stokes and anti-Stokes bands in the Raman spectra of *p*-nitroanisole and mesitylene. The overall heating of the system was faster at higher concentrations of the polar solute, as would be expected, but selective microwave heating was greater at the lower concentrations that we examined, consistent with Kirkwood *g* values and greater antiparallel dipolar alignment at the higher concentrations. For the solution of 1:20 pNA:mesitylene, microwave heating at 300 W until the solution began to boil produced a temperature differential (ΔT) of 114 °C as determined from the Raman spectra, with the temperature of pNA being 272 °C and mesitylene being 158 °C. The agglomerates were examined by small-angle neutron scattering and estimated to be on the order of ∼600 Å (60 nm) in radius and thus having a volume slightly less than 1 attoliter (10^{-18} L) at 20 °C. Similar results were observed at other solute:solvent ratios; these are the first direct measurements of the origin and magnitude of the selective microwave heating process. Most intriguingly, the large temperature differentials produced by selective microwave heating persisted for many seconds after the microwave source was turned off and as the solutions cooled. This persistent ΔT can be replicated by COMSOL simulations in which the polar agglomerate is treated as a separate phase insulated from the bulk solvent. As the agglomerates are at temperatures considerably above the solvent boiling point, they likely produce a solvent vapor barrier between the agglomerate and the bulk solvent, which insulates the agglomerate and slows the heat-transfer process. This microwave-specific phenomenon has not been identified previously to the best of our knowledge. It brings greater clarity to previous observations involving chemical reactions of polar solutes in nonpolar solvents at or near the solvent boiling point and using dynamic heating profiles, and it can guide the design of future reaction systems aimed at maximizing selective microwave heating. Notably, however, this phenomenon is not likely to translate to solutions of weakly absorbing and/or well solvated solutes in polar solvents, as it is linked here to poorly solvated, polar agglomerates in a nonpolar (largely microwave-transparent) solvent. The attoliter-scale temperature differentials and heat-transfer physics under dynamic microwave heating merit further investigation. Meanwhile, the large and persistent temperature differentials measured here under dynamic microwave heating create opportunities to apply selective microwave heating strategically in chemical synthesis and reaction methodology, which is also a focus of ongoing and future work.

ASSOCIATED CONTENT

Supporting Information

The Supporting Information is available free of charge at https://pubs.acs.org/doi/10.1021/acs.jpcb.0c10291.

Small-angle neutron scattering methods and characterization of the aggregates; static dielectric measurements and the determination of the dipole moments in the solution of aggregates; microwave instrumentation and heating protocols of the aggregate solutions; Raman instrumentation and the methodology of the collection of Stokes and anti-Stokes Raman spectra on the aggregate solutions under dynamic microwave heating; analysis of the Raman data to extract the effective temperature of the aggregates and the solvent; COMSOL modeling of the heat transfer processes (PDF)

AUTHOR INFORMATION

Corresponding Authors

Gregory B. Dudley − *C. Eugene Bennett Department of Chemistry, West Virginia University, Morgantown, West Virginia 26506, United States;* orcid.org/0000-0001-6133-3747; Email: gregory.dudley@mail.wvu.edu

A. E. Stiegman − *Department of Chemistry and Biochemistry, Florida State University, Tallahassee, Florida 32312, United States;* orcid.org/0000-0002-8307-0877; Email: stiegman@chem.fsu.edu

Authors

Yuchuan Tao − *Department of Chemistry and Biochemistry, Florida State University, Tallahassee, Florida 32312, United States*

Chong Teng − *Department of Chemistry and Biochemistry, Florida State University, Tallahassee, Florida 32312, United States*

Terence D. Musho − *Department of Mechanical & Aerospace Engineering, West Virginia University, Morgantown, West Virginia 26506, United States*

Lambertus van de Burgt − *Department of Chemistry and Biochemistry, Florida State University, Tallahassee, Florida 32312, United States*

Eric Lochner − *Department of Physics, Florida State University, Tallahassee, Florida 32312, United States*

William T. Heller − *Neutron Scattering Division, Oak Ridge National Laboratory, Oak Ridge, Tennessee 37831, United States;* orcid.org/0000-0001-6456-2975

Geoffrey F. Strouse − *Department of Chemistry and Biochemistry, Florida State University, Tallahassee, Florida 32312, United States;* orcid.org/0000-0003-0841-282X

Complete contact information is available at: https://pubs.acs.org/10.1021/acs.jpcb.0c10291

Notes

The authors declare no competing financial interest.

■ ACKNOWLEDGMENTS

The National Science Foundation under Grant NSF CHE 1665029 provided funding for this work. We also thank CEM Corporation for their technical support. A portion of this research used resources at the Spallation Neutron Source, a DOE Office of Science User Facility operated by the Oak Ridge National Laboratory.

■ REFERENCES

(1) Mingos, D. M. P.; Baghurst, D. R. Applications of Microwave Dielectric Heating Effects to Synthetic Problems in Chemistry. *Chem. Soc. Rev.* **1991**, *20*, 1−47.

(2) Kappe, C. O. Microwave Dielectric Heating in Synthetic Organic Chemistry. *Chem. Soc. Rev.* **2008**, *37*, 1127−1139.

(3) Kappe, C. O.; Dallinger, D.; Murphree, S. *Practical Microwave Synthesis for Organic Chemists: Strategies, Instruments, and Protocols*; Wiley-VCH: Weinheim, 2009; p 299.

(4) Loupy, A. *Microwaves in Organic Synthesis*, 1st ed.; Wiley-VCH: Weinheim, 2006; Vol. *1*, p 532.

(5) Loupy, A. *Microwaes in Organic Synthesis*, 1st ed.; Wiley-VCH: Weinheim, 2006; Vol. *2*.

(6) Koshima, H.; Kubota, M. High-Throughput Synthesis of Alkylbenzophenones with Indium Triflate in the Absence of Solvents Using Microwave. *Synth. Commun.* **2003**, *33*, 3983−3988.

(7) Learmonth, D. A. Rapid Microwave-Promoted Synthesis of Functionalised Benzophenones. *Synth. Commun.* **2002**, *32*, 2757−2762.

(8) Stuerga, D.; Gonon, K.; Lallemant, M. Microwave-Heating as a New Way to Induce Selectivity between Competitive Reactions - Application to Isomeric Ratio Control in Sulfonation of Naphthalene. *Tetrahedron* **1993**, *49*, 6229−6234.

(9) Dudley, G. B.; Stiegman, A. E.; Rosana, M. R. Correspondence on Microwave Effects in Organic Synthesis. *Angew. Chem., Int. Ed.* **2013**, *52*, 7918−7923.

(10) Rosana, M. R.; Hunt, J.; Ferrari, A.; Southworth, T. A.; Tao, Y.; Stiegman, A. E.; Dudley, G. B. Microwave-Specific Acceleration of a Friedel-Crafts Reaction: Evidence for Selective Heating in Homogeneous Solution. *J. Org. Chem.* **2014**, *79*, 7437−7450.

(11) Rosana, M. R.; Tao, Y.; Stiegman, A. E.; Dudley, G. B. On the Rational Design of Microwave-Actuated Organic Reactions. *Chemical Science* **2012**, *3*, 1240−1244.

(12) Kikuchi, S.; Tsubo, T.; Ashizawa, T.; Yamada, T. Extraordinary Effect of Microwave Irradiation on Asymmetric Catalysis. *Chem. Lett.* **2010**, *39*, 574−575.

(13) Nushiro, K.; Kikuchi, S.; Yamada, T. Microwave Effect on Catalytic Enantioselective Claisen Rearrangement. *Chem. Commun.* **2013**, *49*, 8371−8373.

(14) Shironita, S.; Takasaki, T.; Kamegawa, T.; Mori, K.; Yamashita, H. Synthesis of Nano-Sized Platinum Metal Particles on Ti-Containing Mesoporous Silica Using Microwave-Assisted Deposition Method. *Top. Catal.* **2010**, *53*, 218−223.

(15) Tsukahara, Y.; Higashi, A.; Yamauchi, T.; Nakamura, T.; Yasuda, M.; Baba, A.; Wada, Y. In Situ Observation of Non-equilibrium Local Heating as an Origin of Special Effect of Microwave on Chemistry. *J. Phys. Chem. C* **2010**, *114*, 8965−8970.

(16) Fulo, H. F.; Vincent, M. A.; Stiegman, A. E.; Dudley, G. B. Cooperative Application of Conventional and Microwave Heating. *Asian J. Org. Chem.* **2020**, *9*, 961−966.

(17) Frasso, M. A.; Stiegman, A. E.; Dudley, G. B. Microwave-Specific Acceleration of a Retro-Diels-Alder Reaction. *Chem. Commun.* **2020**, *56*, 11247−11250.

(18) de la Hoz, A.; Diaz-Ortiz, A.; Moreno, A. Selectivity under the Action of Microwave Irradiation. In *Microwaves in Organic Synthesis*; Loupy, A., Ed.; Wiley-VCH: Weinheim, 2006; Vol. *1*, pp 219−277.

(19) Hajek, M. Microwave Catalysis in Organic Synthesis. In *Microwaves in Organic Synthesis*, Loupy, A., Ed. Wiley-VCH: Weinheim, 2002; Vol. *1*, pp 345−374.

(20) Steinreiber, A.; Stadler, A.; Mayer, S. F.; Faber, K.; Kappe, C. O. High-Speed Microwave-Promoted Mitsunobu Inversions. Application toward the Deracemization of Sulcatol. *Tetrahedron Lett.* **2001**, *42*, 6283−6286.

(21) Perreux, L.; Loupy, A. A Tentative Rationalization of Microwave Effects in Organic Synthesis According to the Reaction Medium, and Mechanistic Considerations. *Tetrahedron* **2001**, *57*, 9199−9223.

(22) Huang, W.; Richert, R. The Physics of Heating by Time-Dependent Fields: Microwaves and Water Revisited. *J. Phys. Chem. B* **2008**, *112*, 9909−9913.

(23) Huang, W.; Richert, R. Dynamics of Glass-Forming Liquids. XIII. Microwave Heating in Slow Motion. *J. Chem. Phys.* **2009**, *130*, 194509.

(24) Wang, L. M.; Richert, R. Exponential Probe Rotation in Glass-Forming Liquids. *J. Chem. Phys.* **2004**, *120*, 11082−11089.

(25) Debye, P. *Polar Molecules*, 1st ed.; Chemical Catalog Company: New York, 1929; p 172.

(26) Gilani, A. G. *Dielectric and Electro-Optical Properties of Some Cyanobiphenyl Liquid Crystals.* Ph.D. Dissertation, University of Ashton, Brimingham, UK, 1995.

(27) Chen, P.-K.; Rosana, M. R.; Dudley, G. B.; Stiegman, A. E. Parameters Affecting the Microwave-Specific Acceleration of a Chemical Reaction. *J. Org. Chem.* **2014**, *79*, 7425−7436.

(28) Sumi, T.; Dillert, R.; Horikoshi, S. Novel Microwave Thermodynamic Model for Alcohol with Clustering Structure in Nonpolar Solution. *J. Phys. Chem. B* **2015**, *119*, 14479−14485.

(29) Wu, Y.; Gagnier, J.; Dudley, G. B.; Stiegman, A. E. The "Chaperone" Effect in Microwave-Driven Reactions. *Chem. Commun.* **2016**, *52*, 11281−11283.

(30) Do, C.; Heller, W. T.; Stanley, C.; Gallmeier, F. X.; Doucet, M.; Smith, G. S. Understanding Inelastically Scattered Neutrons from Water on a Time-of-Flight Small-Angle Neutron Scattering (Sans) Instrument. *Nucl. Instrum. Methods Phys. Res., Sect. A* **2014**, *737*, 42−46.

(31) Guggenheim, E. A. A Proposed Simplification in the Procedure for Computing Electric Dipole Moments. *Trans. Faraday Soc.* **1949**, *45*, 714−720.

(32) Guggenheim, E. A. The Computation of Electric Dipole Moments. *Trans. Faraday Soc.* **1951**, *47*, 573−576.

(33) Gilani, A. G.; Mamaghani, M.; Anbir, L. Dipole Moments and Intermolecular Association of Some Carbonyl Compounds in Nonpolar Solvents. *J. Solution Chem.* **2003**, *32*, 625−636.
(34) Musho, T. D.; Wildfire, C.; Houlihan, N. M.; Sabolsky, E. M.; Shekhawat, D. Study of Cu2o Particle Morphology on Microwave Field Enhancement. *Mater. Chem. Phys.* **2018**, *216*, 278−284.
(35) Herman, I. P. Peak Temperatures from Raman Stokes/Anti-Stokes Ratios During Laser Heating by a Gaussian Beam. *J. Appl. Phys.* **2011**, *109*, 016103.
(36) Moore, D. S.; McGrane, S. D. Raman Temperature Measurement. *Journal of Physics: Conference Series* **2014**, *500*, 192011.
(37) Long, D. A. *Raman Spectroscopy*, 1st ed.; MacGraw-Hill: New York, 1977; p 276.
(38) Trisaksri, V.; Wongwises, S. Critical Review of Heat Transfer Characteristics of Nanofluids. *Renewable Sustainable Energy Rev.* **2007**, *11*, 512−523.
(39) Patel, H. E.; Das, S. K.; Sundararajan, T.; Sreekumaran Nair, A.; George, B.; Pradeep, T. Thermal Conductivities of Naked and Monolayer Protected Metal Nanoparticle Based Nanofluids: Manifestation of Anomalous Enhancement and Chemical Effects. *Appl. Phys. Lett.* **2003**, *83*, 2931−2933.

https://dx.doi.org/10.1021/acs.jpcb.0c10291
J. Phys. Chem. B 2021, 125, 2146−2156